Entanglement concentration of continuous-variable quantum states

Jaromír Fiurášek, Ladislav Mišta, Jr., and Radim Filip
Department of Optics, Palacký University, 17. listopadu 50, 77200 Olomouc, Czech Republic
(Received 31 May 2002; published 13 February 2003)

We propose two probabilistic entanglement concentration schemes for a single copy of a two-mode squeezed vacuum state. The first scheme is based on the off-resonant interaction of a Rydberg atom with the cavity field while the second setup involves the cross Kerr interaction, an auxiliary mode prepared in a strong coherent state, and homodyne detection. We show that the continuous-variable entanglement concentration allows us to improve the fidelity of teleportation of coherent states.

DOI: 10.1103/PhysRevA.67.022304 PACS number(s): 03.67.−a, 42.50.Dv

I. INTRODUCTION

Quantum entanglement is an essential ingredient of many protocols for quantum information processing such as quantum teleportation [1,2] or quantum cryptography [3]. In order to achieve optimum performance of these protocols, the two involved parties, traditionally called Alice and Bob, should share a pure maximally entangled state. In practice, however, we are often able to generate only nonmaximally entangled states. Additionally, the distribution of the entangled state between the two distant parties via some noisy quantum channel will degrade the entanglement and Alice and Bob will share some partially entangled mixed state. One of the most important discoveries in quantum information theory was the development of the entanglement distillation protocols that allow Alice and Bob to extract a small number of highly entangled almost pure states from a large number of weakly entangled mixed states [4–6]. These protocols involve only local operations and classical communication (LOCC) between the two parties; therefore they can be performed after the distribution of the entangled states.

In the simplest scenario Alice and Bob share a pure nonmaximally entangled state in a d-dimensional Hilbert space whose Schmidt decomposition reads

$$|\psi\rangle=\sum_{j=1}^{d} c_j|a_j\rangle_A|b_j\rangle_B, \tag{1}$$

where each set of states $|a_j\rangle$ and $|b_j\rangle$ forms a basis. Alice and Bob would like to prepare from $|\psi\rangle$ a state with higher entanglement by means of LOCC. Remarkably, this is possible, albeit only with certain probability, even if they share only a single copy of this state. The procedure that accomplishes this task was fittingly called the procrustean method [4], because it cuts off the Schmidt coefficients c_j to the size of the smallest one. In this way, Alice and Bob obtain, with certain probability, a maximally entangled state in a d-dimensional Hilbert space.

In view of the recent interest in quantum information processing with continuous variables [2,7–10], it is highly desirable to establish experimentally feasible entanglement distillation and concentration protocols for continuous variables. Of particular importance are the protocols for Gaussian states, because these states can be prepared in the laboratory with the use of commonly available resources comprising lasers, passive linear optical elements (beam splitters and phase shifters), and optical parametric amplifiers. Recall that the Wigner function of a Gaussian state exhibits Gaussian shape. If we employ also auxiliary modes prepared initially in some Gaussian state and homodyne detectors, then we can implement an arbitrary Gaussian completely positive map [11–13], which is a transformation that preserves the Gaussian shape of the Wigner function. However, it was proved recently that it is impossible to distill Gaussian entangled states by means of Gaussian operations [14]. This means that additional resources beyond passive linear optics, optical parametric amplifiers, and homodyne detectors are required.

The distillation protocols for Gaussian states proposed so far employ photon-number measurements. The scheme suggested by Duan *et al.* [15] relies on nondemolition measurement of the total photon number in two (or more) modes and represents a direct extension of the Schmidt projection method to infinite-dimensional Hilbert space. The procrustean scheme considered by Opatrný *et al.* [16] and further analyzed by Cochrane *et al.* [17] is based on controlled addition or subtraction of photons. In this scheme, the nonlinearity required to implement a non-Gaussian transformation is induced by a measurement that should resolve the number of photons in the mode. This is in the spirit of the recent proposal of efficient quantum computation with linear optics [18] where the measurement-induced nonlinearity plays a central role. We also note that several distillation schemes for entangled coherent states have been proposed [19,20].

In this paper, we design two entanglement-concentration setups for a single copy of a pure two-mode squeezed vacuum state

$$|\psi\rangle=\sum_{n=0}^{\infty} c_n|n,n\rangle, \qquad c_n=\sqrt{1-\lambda^2}\lambda^n, \tag{2}$$

where $\lambda=\tanh r$ and r is the squeezing constant. This state can be generated in the process of a nondegenerate spontaneous parametric down-conversion and represents a common source of continuous-variable entanglement in the experiments. The procrustean procedures that we are proposing preserve the structure of the state (2) while the Schmidt coefficients c_n are transformed to different ones, $c_n \to d_n$. The first scheme is based on a dispersive interaction of a two-level atom with the microwave cavity field and atomic state

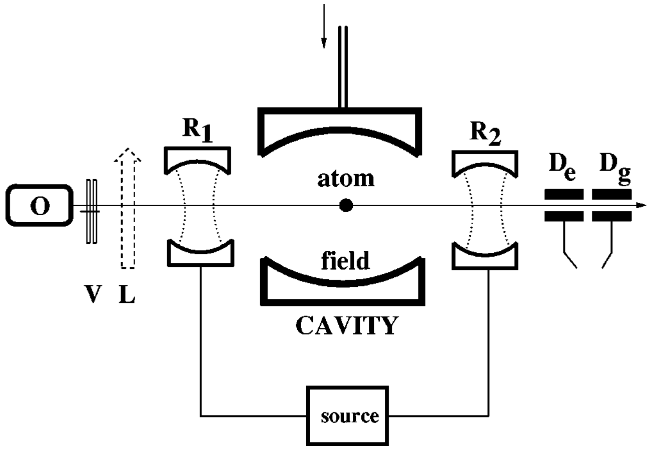

FIG. 1. Schematic of entanglement-concentration setup in cavity QED: O is the atomic oven, V is the atomic velocity selector, L is the laser excitation mechanism, R_1 and R_2 are the Ramsey zones driven by the microwave source, CAVITY contains Alice's part of the entangled state, and D_e, D_g are the field ionization detectors measuring the state of the Rydberg atom.

detection. The second scheme utilizes a cross Kerr interaction, coherent states, homodyne measurements, and linear optics. The underlying mechanism of both these schemes is that a certain auxiliary system experiences a phase shift that depends on the number of photons in Alice's mode of the shared state (2). We convert this phase modulation into amplitude modulation via interference, which allows us to control the amplitude of the Schmidt coefficients c_n. An essential part of our probabilistic protocols is the measurement on the auxiliary system which tells us whether the concentration succeeded or failed.

The paper is organized as follows. The first scheme is analyzed in Sec. II and the second scheme is discussed in Sec. III. Finally, Sec. IV contains the conclusions.

II. ENTANGLEMENT CONCENTRATION IN CAVITY QUANTUM ELECTRODYNAMICS

Our first entanglement concentration scheme is designed for the quantum state of an electromagnetic field confined in a high-Q cavity and is schematically sketched in Fig. 1. Note that this setup has been successfully realized experimentally and employed for quantum nondemolition measurements of the cavity-field photon number and the preparation of Schrödinger cat states [21,22]. The scheme shown in Fig. 1 is based on an off-resonant interaction of an (effectively) two-level Rydberg atom with a single mode of a cavity sandwiched in the Ramsey interferometer. Alice's part of the two-mode entangled state is transmitted to the cavity through a superconducting waveguide [23]. The atoms are emitted from an oven, their velocity is selected by a velocity selector, and they are excited by a laser pulse to the long-living circular Rydberg state $|g\rangle$. Subsequently, each atom enters the first microwave Ramsey zone where a strong coherent microwave field resonantly drives the atomic transition between two Rydberg states $|g\rangle$ and $|e\rangle$. The atom leaves the Ramsey zone R_1 in a balanced coherent superposition of the states $|g\rangle$ and $|e\rangle$,

$$|\phi\rangle = \frac{1}{\sqrt{2}}(|g\rangle + |e\rangle). \tag{3}$$

The atom then traverses the cavity that contains Alice's part of the shared two-mode state (2). The dispersive atom-field interaction in the cavity is governed by the following effective Hamiltonian [21]:

$$H = \hbar\kappa a^\dagger a \otimes |e\rangle\langle e|, \tag{4}$$

where a is the annihilation operator of Alice's mode and κ is the effective atom-field interaction constant. The coupling (4) results in a phase shift $\Delta\varphi = a^\dagger a\varphi$ of the state $|e\rangle$ that is linearly proportional to the number of photons in the mode A. On the other hand, the state $|g\rangle$ is not changed by the interaction. The single-photon phase shift $\varphi = \kappa t$, where t is an effective interaction time, can be adjusted to the required value by a proper selection of the atomic velocity in the selector V.

After leaving the central cavity, the atom passes through the second microwave Ramsey zone, where it undergoes a $\pi/2$ Rabi rotation. In general, the frequency ω_r of the classical microwave field differs slightly from the atomic transition frequency ω_0. This results in a change of the relative phase between the atomic coherence and the microwave source by an angle

$$\varphi_0 = (\omega_r - \omega_0)T, \tag{5}$$

where T is the time of flight of the atom between the zones R_1 and R_2 [24]. The transformation undergone by the atom in zone R_2 can be written as follows:

$$|g\rangle \rightarrow \frac{1}{\sqrt{2}}(|g\rangle + e^{-i\varphi_0}|e\rangle),$$

$$|e\rangle \rightarrow \frac{1}{\sqrt{2}}(|e\rangle - e^{i\varphi_0}|g\rangle). \tag{6}$$

The phase shift φ_0 can be controlled by tuning the frequency ω_r of the microwave field [see Eq. (5)].

The resulting state of the atom and the two-mode field reads

$$|\Psi\rangle = \frac{1}{2}\sum_{n=0}^{\infty} c_n(1 - e^{i\varphi_0 - in\varphi})|g\rangle \otimes |n,n\rangle + \frac{1}{2}\sum_{n=0}^{\infty} c_n(e^{-i\varphi_0} + e^{-in\varphi})|e\rangle \otimes |n,n\rangle. \tag{7}$$

To complete the procedure, we measure the state of the atom by means of state-selective ionization detectors D_g and D_e exhibiting almost unit detection efficiency. The entanglement concentration succeeds only if the atom is found to be in the ground state $|g\rangle$. The Schmidt coefficients after this conditional transformation read

$$d_n = i c_n \exp\left(i\frac{\varphi_0 - n\varphi}{2}\right)\sin\left(\frac{n\varphi-\varphi_0}{2}\right). \tag{8}$$

The irrelevant overall phase factor $i\exp(i\varphi_0/2)$ can be dropped. Moreover, the phase factor $\exp(-in\varphi/2)$ can easily be compensated by an appropriate phase shift or simply by properly redefining the quadratures of Alice's mode. After these transformations, the Schmidt coefficients become real and after renormalization we get

$$d_n = \sqrt{\frac{1-\lambda^2}{P}}\ \lambda^n \sin\left(\frac{n\varphi-\varphi_0}{2}\right), \tag{9}$$

where

$$P = \frac{1}{2} - \frac{1-\lambda^2}{2}\,\frac{\cos\varphi_0 - \lambda^2\cos(\varphi+\varphi_0)}{1-2\lambda^2\cos\varphi+\lambda^4} \tag{10}$$

is the probability of success of the conditional transformation. Clearly, two trends are competing in Eq. (9). The exponential decay λ^n (recall that $|\lambda|<1$) is for certain n partially compensated by the second term $\sin[(n\varphi-\varphi_0)/2]$ which grows with n up to $n_{\max}=(\pi+\varphi_0)/\varphi$. This allows us to increase the entanglement of the shared state.

Formally, the conditional transformation can be described as a diagonal filter applied to the input two-mode density matrix $\rho_{\rm in}$. We define an operator

$$A = \sum_{n=0}^{\infty} a_n |n\rangle\langle n|, \tag{11}$$

where $a_n = \sin[(n\varphi-\varphi_0)/2]$. The output (unnormalized) density matrix is given by

$$\rho_{\rm out} = A\otimes \mathbb{1}_B \rho_{\rm in} A^\dagger \otimes \mathbb{1}_B, \tag{12}$$

where $\mathbb{1}_B$ stands for an identity operator in the Hilbert space of Bob's mode.

Since the conditional transformation (12) preserves the purity of the two-mode state, we can conveniently quantify the entanglement by the von Neumann entropy of the reduced density matrix of Alice's mode,

$$S = -\sum_{n=0}^{\infty} |d_n^2| \ln |d_n^2|. \tag{13}$$

The entropy S is plotted in Fig. 2(a) as a function of φ_0 for fixed φ and λ. Before concentration, Alice and Bob share the two-mode squeezed vacuum (2), and the entropy (13) reads

$$S = -\ln(1-\lambda^2) - \frac{\lambda^2}{1-\lambda^2}\ln\lambda^2. \tag{14}$$

For the data in Fig. 2, we obtain $S_{\rm in}=0.75$. Figure 2(a) clearly shows that for certain interval of phase shifts φ_0 our procedure allows us to conditionally increase the amount of entanglement in the pure two-mode state shared by Alice and Bob.

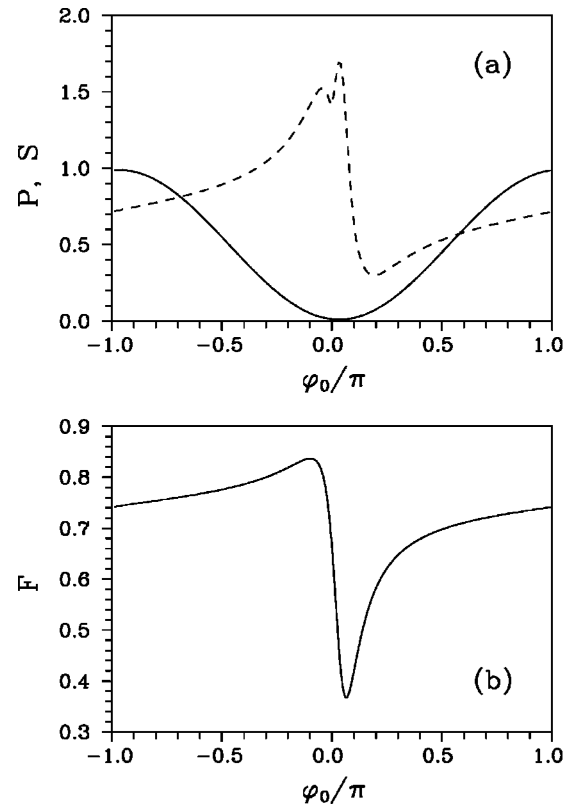

FIG. 2. The performance of the entanglement-concentration scheme shown in Fig. 1 for $\lambda=1/2$ and $\varphi=\pi/10$. (a) Probability of success P (solid line) and von Neumann entropy S after the concentration (dashed line) and (b) fidelity F of teleportation of coherent states are plotted as functions of φ_0. For the input state, $S_{\rm in}=0.75$ and $F_{\rm in}=0.75$.

Let us now demonstrate that the entanglement concentrated in this way is useful in practical tasks. To be specific, we consider the teleportation of coherent states in the Braunstein-Kimble scheme [2] where our state is used as the quantum channel. Making use of the transfer operator formalism [25,26], we can express the fidelity of teleportation as follows:

$$F = \frac{1}{2}\sum_{m=0}^{\infty}\sum_{n=0}^{\infty}\binom{m+n}{n}\frac{d_m d_n^*}{2^{m+n}}. \tag{15}$$

On inserting the Schmidt coefficients (9) into Eq. (15) and carrying out the summations we obtain an analytical formula for the fidelity of teleportation of coherent states,

$$F = \frac{1-\lambda^2}{4P}\left[\frac{1}{1-\lambda\cos(\varphi/2)} - \frac{\cos\varphi_0 - \lambda\cos(\varphi/2+\varphi_0)}{1-2\lambda\cos(\varphi/2)+\lambda^2}\right]. \tag{16}$$

The fidelity F is plotted in Fig. 2(b). For fixed λ and φ we can optimize the phase φ_0 so that the teleportation fidelity F will be maximized. For the data used in Fig. 2, we find that it is optimum to set $\varphi_0 \approx -\pi/10$, which yields the fidelity $F=0.837$ and the probability of success is $P=0.05$. This should be compared with the fidelity $F_{\rm in}=0.75$ that is

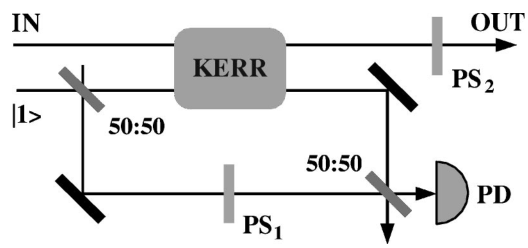

FIG. 3. Optical implementation of the entanglement-concentration scheme shown in Fig. 1.

achieved when the original two-mode squeezed vacuum with $\lambda = 1/2$ serves as the quantum channel. This improvement in fidelity is quite significant and clearly illustrates the practical utility of our procedure.

III. ENTANGLEMENT CONCENTRATION FOR TRAVELING LIGHT FIELDS

To implement the scheme discussed in the preceding section directly for traveling light fields, we could replace the atomic Ramsey interferometer with a Mach-Zehnder interferometer for a single photon and couple this auxiliary photon to Alice's mode via a nonlinear medium using the cross Kerr effect (see Fig. 3). A similar setup was proposed by Gerry for the generation of Schrödinger cat states [27]. However, this scheme has several drawbacks. First, the currently achievable Kerr nonlinearities are rather low. Secondly, we have to prepare a single photon. Therefore we propose an alternative scheme (see Fig. 4). In that setup, an auxiliary mode C is prepared in a (strong) coherent state $|\alpha\rangle$ and then interacts with Alice's mode A in the Kerr medium described by the Hamiltonian

$$H_{\mathrm{Kerr}} = \hbar \kappa a^{\dagger} a c^{\dagger} c, \tag{17}$$

where a and c denote the annihilation operators of Alice's and the auxiliary modes, respectively. After the interaction, we project the output state onto coherent state $|\beta\rangle$ in the eight-port homodyne detector (EHD).

The principle of the operation of this scheme may be explained as follows. If there are n photons in the mode A, then the coherent state $|\alpha\rangle$ evolves to $|\alpha e^{in\varphi}\rangle$, where $\varphi = -\kappa t$ and t is the effective interaction time. The probability density of projecting onto $|\beta\rangle$ is given by $|\langle\beta|\alpha e^{in\varphi}\rangle|^2/\pi$ which may grow with n if β belongs to a certain region of the phase space. Without loss of generality, we may assume that α is

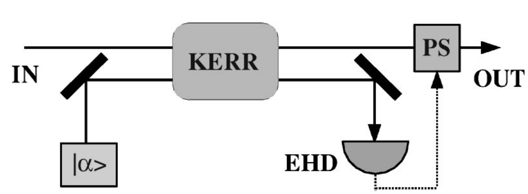

FIG. 4. Schematic of the entanglement-concentration setup for traveling light fields that is based on auxiliary coherent states, the cross Kerr interaction, eight-port homodyne detection (EHD), and a linear phase shift (PS) depending on the outcome of the measurement.

real and positive and define $\beta = |\beta| \exp(i\varphi_0)$. After projecting onto β, the Schmidt coefficients can be expressed as

$$d_n = \frac{\langle\beta|\alpha e^{in\varphi}\rangle}{\sqrt{\pi Q(\beta)}} c_n. \tag{18}$$

The normalization factor $Q(\beta)$ represents the total probability density that β will be measured in the EHD,

$$Q(\beta) = \frac{1}{\pi} \sum_{n=0}^{\infty} |\langle\beta|\alpha e^{in\varphi}\rangle|^2 |c_n|^2.$$

Making use of the formula for the scalar product of two coherent states [28]

$$\langle\beta|\alpha\rangle = \exp\left(-\frac{1}{2}|\alpha|^2 - \frac{1}{2}|\beta|^2 + \beta^* \alpha\right) \tag{19}$$

and assuming that Alice and Bob initially share the two-mode squeezed vacuum state (2) we obtain

$$Q(\beta) = \frac{1-\lambda^2}{\pi} \sum_{n=0}^{\infty} \lambda^{2n} \exp(-|\alpha e^{in\varphi} - \beta|^2). \tag{20}$$

It is convenient to express the Schmidt coefficients d_n in terms of two real parameters q_n and ϕ_n,

$$d_n = \frac{c_n}{\sqrt{\pi Q(\beta)}} \exp\left(q_n + i\phi_n - \frac{1}{2}|\alpha|^2 - \frac{1}{2}|\beta|^2\right), \tag{21}$$

where

$$q_n = |\alpha\beta| \cos(n\varphi - \varphi_0), \tag{22}$$

$$\phi_n = |\alpha\beta| \sin(n\varphi - \varphi_0). \tag{23}$$

We can see from Eq. (21) that the amplitude of the old Schmidt coefficients c_n is modulated by the factors $\exp(q_n)$. The highest relative enhancement occurs for $n = \varphi_0/\varphi$, when $q_n = |\alpha\beta|$. Since the nonlinear phase shift $n\varphi$ will typically be very small for all n for which c_n substantially differs from zero, $|\alpha| n\varphi \ll 1$, we can expand the expressions (22) and (23) in Taylor series and keep only terms up to linear in $n\varphi$,

$$q_n = |\alpha\beta| \cos\varphi_0 + n\varphi|\alpha\beta| \sin\varphi_0,$$
$$\phi_n = -|\alpha\beta| \sin\varphi_0 + n\varphi|\alpha\beta| \cos\varphi_0. \tag{24}$$

Within this approximation the exponents q_n are linearly proportional to n and the conditional transformation preserves the structure of the two-mode squeezed state:

$$|d_n| \propto \tilde{\lambda}^n, \quad \tilde{\lambda} = \lambda \exp(\varphi|\alpha\beta| \sin\varphi_0). \tag{25}$$

For small nonlinear phase shifts $\varphi \ll \pi$ the distribution $Q(\beta)$ is almost identical to the input Gaussian distribution $Q_{\mathrm{in}}(\beta) = \exp(-|\alpha-\beta|^2)/\pi$ [see Fig. 5(a)]. For all β that can be detected with some significantly large probability the imaginary part of β will thus be of the order of unity or lower, $-1 \lesssim |\beta| \sin\varphi_0 \lesssim 1$. It follows from Eqs. (24) and (25)

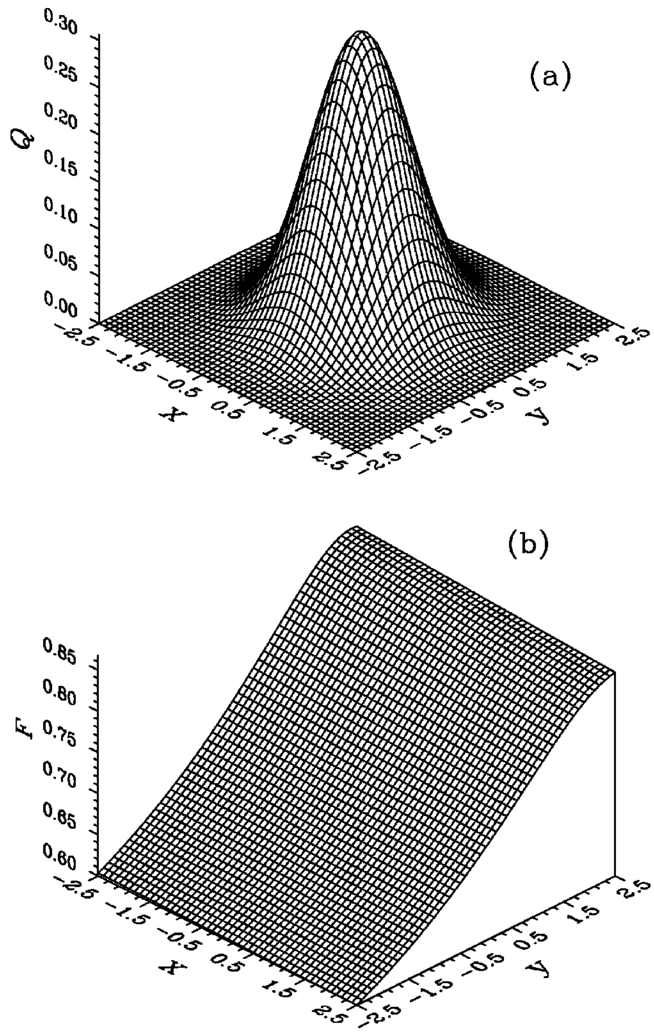

FIG. 5. (a) The Q function $Q(\beta)$ of the output state of the auxiliary mode and (b) the fidelity $F(\beta)$ are shown for $\lambda=1/2$, $\alpha=10$, $\varphi=\pi/100$. The coordinates x and y are defined as $x+iy=\beta-\alpha$.

that the product $\varphi|\alpha|$ effectively determines the modulation of the Schmidt coefficients. An important advantage of our scheme is that a weak Kerr nonlinearity (small phase shift φ) can be compensated by using a sufficiently strong auxiliary coherent state with $\alpha \propto 1/\varphi$. Thus the mean number of photons in the auxiliary mode should be proportional to the inverse square of the nonlinear phase shift, $|\alpha|^2 \propto 1/\varphi^2$. In order to keep the intensity of the auxiliary mode at a reasonable level, we still need a quite strong nonlinear phase shift (e.g., $\varphi=\pi/100$). Note that, although such a phase shift may seem to be modest, it is in fact very large and common nonresonant media typically exhibit a third-order nonlinearity that is weaker by several orders of magnitude. Recently, however, it was shown that the strength of the cross Kerr interaction can be enhanced by many orders of magnitude in a coherently prepared resonant atomic medium. A medium with electromagnetically induced transparency can exhibit very large Kerr nonlinearity [29–33] that would suffice for the practical implementation of the present entanglement-concentration scheme.

One undesirable effect of the projection onto the coherent state $|\beta\rangle$ is the phase modulation ϕ_n of the Schmidt coefficients (23). However, if the approximation (24) holds then the conditional phase shift ϕ_n is linearly proportional to n and can be removed by a suitable phase shifter PS. The actual phase shift is proportional to the real part of β and we must use a feedforward scheme, where the operation of the PS (e.g., a Pockels cell) is controlled by the measurement outcome, as is schematically indicated in Fig. 4.

After the compensation of the linear phase shift $\varphi|\alpha\beta|\cos\varphi_0$, the normalized Schmidt coefficients corresponding to the measurement outcome β read

$$d_n(\beta)=\frac{\sqrt{1-\lambda^2}\lambda^n \exp[\alpha\beta^* e^{in\varphi}-in\varphi|\alpha\beta|\cos\varphi_0]}{\sqrt{\pi Q(\beta)}\exp(|\alpha|^2/2+|\beta|^2/2)}. \tag{26}$$

We need to establish a criterion according to which we will accept or reject the state depending on the measurement outcome β. The most natural approach is to choose some reasonable figure of merit $F(\beta)$ that has to be evaluated for each β and then specify a region Ω in the phase space where this figure of merit is sufficiently large. The entanglement concentration succeeds only if $\beta \in \Omega$ and fails otherwise. It follows that the concentration will yield a mixture of the states

$$|\psi(\beta)\rangle=\sum_{n=0}^{\infty} d_n(\beta)|n,n\rangle \tag{27}$$

and the density matrix of the output state shared by Alice and Bob can be expressed as follows:

$$\rho_\Omega=\frac{1}{P_\Omega}\int_\Omega d^2\beta \;\; Q(\beta)|\psi(\beta)\rangle\langle\psi(\beta)|. \tag{28}$$

Here

$$P_\Omega=\int_\Omega d^2\beta \;\; Q(\beta) \tag{29}$$

denotes the probability of success of the concentration, i.e., the probability that the measurement outcome β will belong to Ω. Different functions $F(\beta)$ may be suitable depending on the intended usage of the shared quantum state. In this paper, we choose the fidelity (15) of the teleportation of coherent states as the figure of merit.

In the rest of this section we present the results of the numerical calculations for $\alpha=10$, $\varphi=\pi/100$, and $\lambda=1/2$. The function $F(\beta)$ is plotted in Fig. 5(b). We can see that there are regions in the phase space where $F(\beta)$ is higher than the fidelity corresponding to the input two-mode squeezed vacuum, $F_{\text{in}}=0.75$. As described above, we define Ω as the region of the phase space where $F(\beta)\geqslant F_{\text{th}}$. The average fidelity associated with the threshold F_{th} can be calculated as follows:

$$F_\Omega=\frac{1}{P_\Omega}\int_\Omega d^2\beta \;\; Q(\beta)F(\beta). \tag{30}$$

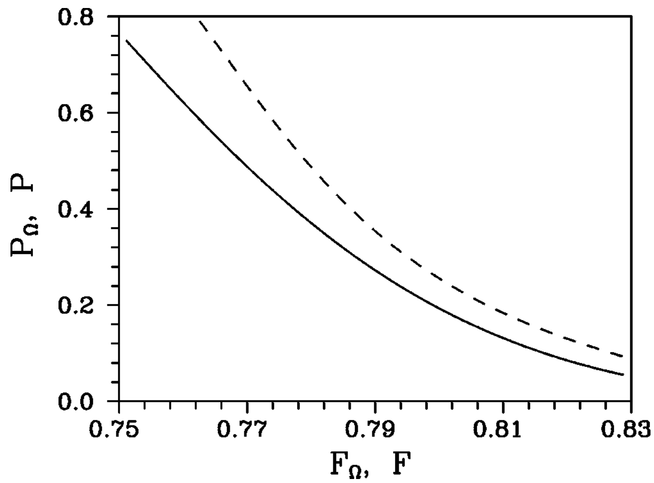

FIG. 6. The probability P_Ω of success of the entanglement concentration is plotted in dependence on the fidelity F_Ω of teleportation of coherent states that can be achieved with the entangled state after the concentration. Solid line represents results for the scheme based on the cross Kerr interaction and depicted in Fig. 4; the parameters are the same as in Fig. 5. For comparison, the dashed line displays the dependence of P on F for the scheme based on cavity QED (see Fig. 1) and all parameters are the same as in Fig. 2.

Figure 6 shows the dependence of the probability of success P_Ω on the average fidelity F_Ω. Recall that with the help of the original two-mode squeezed vacuum we can achieve the fidelity $F_{\mathrm{in}}=0.75$. As can be seen from Fig. 6, the present entanglement-concentration method leads to higher fidelities while keeping the probability of successful concentration reasonably high. For instance, the probability of entanglement concentration yielding $F_\Omega=0.8$ reads $P_\Omega\approx 0.2$. This example confirms that our procedure indeed extracts more useful entanglement from the input two-mode squeezed vacuum.

Finally, let us compare the two schemes proposed in Secs. II and III of this paper. A general comparison of these two setups is not easy because they both involve several free parameters that can be varied and, possibly, optimized. However, the two schemes are qualitatively similar in the formal sense. The transformation of the entangled state has in both cases the structure given by Eqs. (11) and (12) although the specific dependence of the coefficients a_n on n differs for these two schemes. An explicit comparison for the particular choice of parameters considered in this paper reveals that both schemes exhibit quite similar performance even on the quantitative level (see Fig. 6 and compare the solid and dashed lines). The main distinction of these two schemes lies in the different physical implementations.

IV. CONCLUSIONS

In this paper, we have designed two schemes for the probabilistic concentration of continuous-variable entanglement. The procrustean protocols that we are proposing have the important property that they can be applied several times to a single copy of the shared two-mode entangled state. Thus we could, in principle, extract a state with very high entanglement, at the expense of a low probability of success. When repeating the concentration procedure, one could optimize the relevant parameters such as the phase shifts φ_0 and φ in order to achieve the optimum performance of the schemes. In view of the recent advances in cavity-QED experiments and the preparation of media with extremely high Kerr nonlinearity, we may hope that the schemes proposed in the present paper will become experimentally feasible in the near future.

ACKNOWLEDGMENTS

This work was supported by an EU grant under the QIPC Project No. IST-1999-13071 (QUICOV) and by Grant No. LN00A015 and Research Project No. CEZ: J14/98: 153100009 ‘‘Wave and Particle Optics’’ of the Czech Ministry of Education.

[1] C.H. Bennett, G. Brassard, C. Crepeau, R. Jozsa, A. Peres, and W.K. Wootters, Phys. Rev. Lett. **70**, 1895 (1993).
[2] L. Vaidman, Phys. Rev. A **49**, 1473 (1994); S.L. Braunstein and H.J. Kimble, Phys. Rev. Lett. **80**, 869 (1998); A. Furusawa, J.L. Sørensen, S.L. Braunstein, C.A. Fuchs, H.J. Kimble, and E.S. Polzik, Science **282**, 706 (1998); T.C. Ralph and P.K. Lam, Phys. Rev. Lett. **81**, 5668 (1998).
[3] A.K. Ekert, Phys. Rev. Lett. **67**, 661 (1991).
[4] C.H. Bennett, H.J. Bernstein, S. Popescu, and B. Schumacher, Phys. Rev. A **53**, 2046 (1996).
[5] C.H. Bennett, G. Brassard, S. Popescu, B. Schumacher, J.A. Smolin, and W.K. Wootters, Phys. Rev. Lett. **76**, 722 (1996).
[6] D. Deutsch, A. Ekert, R. Jozsa, C. Macchiavello, S. Popescu, and A. Sanpera, Phys. Rev. Lett. **77**, 2818 (1996).
[7] G. Lindblad, J. Phys. A **33**, 5059 (2000); N.J. Cerf, A. Ipe, and X. Rottenberg, Phys. Rev. Lett. **85**, 1754 (2000); J. Fiurášek, *ibid.* **86**, 4942 (2001); S.L. Braunstein, N.J. Cerf, S. Iblisdir, P. van Loock, and S. Massar, *ibid.* **86**, 4938 (2001).
[8] S.L. Braunstein, Phys. Rev. Lett. **80**, 4084 (1998); Nature (London) **394**, 47 (1998); S. Lloyd and J.J.E. Slotine, Phys. Rev. Lett. **80**, 4088 (1998).
[9] T.C. Ralph, Phys. Rev. A **61**, 010303(R) (2000); M. Hillery, *ibid.* **61**, 022309 (2000); N.J. Cerf, M. Levy, and G. Van Assche, *ibid.* **63**, 052311 (2001); F. Grosshans and P. Grangier, Phys. Rev. Lett. **88**, 057902 (2002); Ch. Silberhorn, N. Korolkova, and G. Leuchs, *ibid.* **88**, 167902 (2002); Ch. Silberhorn, T.C. Ralph, N. Lütkenhaus, and G. Leuchs, *ibid.* **89**, 167901 (2002).
[10] P. van Loock and S.L. Braunstein, Phys. Rev. A **61**, 010302(R) (1999); S.M. Tan, *ibid.* **60**, 2752 (1999).
[11] B. Demoen, O. Vanheuverzwijn, and A. Verbeure, Lett. Math. Phys. **2**, 161 (1977); Rep. Math. Phys. **15**, 27 (1979).

[12] J. Eisert and M.B. Plenio, Phys. Rev. Lett. **89**, 097901 (2002).
[13] J. Fiurášek, Phys. Rev. A **66**, 012304 (2002).
[14] J. Eisert, S. Scheel, and M.B. Plenio, Phys. Rev. Lett. **89**, 137903 (2002); J. Fiurášek, *ibid.* **89**, 137904 (2002); G. Giedke and J.I. Cirac, Phys. Rev. A **66**, 032316 (2002); R. Filip and L. Mišta, Jr., e-print quant-ph/0204105.
[15] L.M. Duan, G. Giedke, J.I. Cirac, and P. Zoller, Phys. Rev. Lett. **84**, 4002 (2000); Phys. Rev. A **62**, 032304 (2000).
[16] T. Opatrný, G. Kurizki, and D.-G. Welsch, Phys. Rev. A **61**, 032302 (2000).
[17] P.T. Cochrane, T.C. Ralph, and G.J. Milburn, Phys. Rev. A **65**, 062306 (2002).
[18] E. Knill, R. Laflamme, and G.J. Milburn, Nature (London) **409**, 46 (2001).
[19] S. Parker, S. Bose, and M.B. Plenio, Phys. Rev. A **61**, 032305 (2000).
[20] J. Clausen, L. Knöll, and D.-G. Welsch, Phys. Rev. A **66**, 062303 (2002).
[21] M. Brune, S. Haroche, J.M. Raimond, L. Davidovich, and N. Zagury, Phys. Rev. A **45**, 5193 (1992).
[22] M. Brune, E. Hagley, J. Dreyer, X. Maitre, A. Maali, C. Wunderlich, J.M. Raimond, and S. Haroche, Phys. Rev. Lett. **77**, 4887 (1996).
[23] J.M. Raimond, M. Brune, and S. Haroche, Phys. Rev. Lett. **79**, 1964 (1997).
[24] X. Maitre *et al.*, J. Mod. Opt. **44**, 2023 (1997).
[25] H.F. Hofmann, T. Ide, T. Kobayashi, and A. Furusawa, Phys. Rev. A **62**, 062304 (2000).
[26] S.I.J. Kurzeja and A.S. Parkins, e-print quant-ph/0201094.
[27] C.C. Gerry, Phys. Rev. A **59**, 4095 (1999).
[28] J. Peřina, *Quantum Statistics of Linear and Nonlinear Optical Phenomena* (Kluwer, Dordrecht, 1991).
[29] H. Schmidt and A. Imamoḡlu, Opt. Lett. **21**, 1936 (1996).
[30] A. Imamoḡlu, H. Schmidt, G. Woods, and M. Deutsch, Phys. Rev. Lett. **79**, 1467 (1997).
[31] L.V. Hau, S.E. Harris, Z. Dutton, and C.H. Behroozi, Nature (London) **397**, 594 (1999).
[32] M.M. Kash *et al.*, Phys. Rev. Lett. **82**, 5229 (1999).
[33] M.D. Lukin and A. Imamoḡlu, Phys. Rev. Lett. **84**, 1419 (2000).